1 *Supplement of*

2 **High-time-resolution chemical composition and source apportionment of PM$_{2.5}$ in northern Chinese cities:**

3 **implications for policy**

4 Yong Zhang[1,2,3], Jie Tian[1,2,4], Qiyuan Wang[1,2,3,4*], Lu Qi[5], Manousos Ioannis Manousakas[5], Yuemei Han[1,4], Weikang

5 Ran[1,2], Yele Sun[6], Huikun Liu[1,2,4], Renjian Zhang[6], Yunfei Wu[6], Tianqu Cui[5], Kaspar Rudolf Daellenbach[5], Jay Gates

6 Slowik[5], André S. H. Prévôt[5], Junji Cao[6*]

7 [1] State Key Laboratory of Loess and Quaternary Geology, Institute of Earth Environment, Chinese Academy

8 of Sciences, Xi'an 710061, China

9 [2] National Observation and Research Station of Regional Ecological Environment Change and

10 Comprehensive Management in the Guanzhong Plain, Shaanxi, Xi'an 710061, China

11 [3] University of Chinese Academy of Sciences, Beijing 100049, China

12 [4] Center for Excellence in Quaternary Science and Global Change, Xi'an 710061, China

13 [5] Laboratory of Atmospheric Chemistry, Paul Scherrer Institute (PSI), Villigen 5232, Switzerland

14 [6] Institute of Atmospheric Physics, Chinese Academy of Sciences, Beijing 100029, China

15 *Correspondence:* wangqy@ieecas.cn (Qiyuan Wang), jjcao@mail.iap.ac.cn (Junji Cao).

Text S1. Selcation of inputted HERM chemical species and its uncertainty calculation

Considering the validity and credibility of monitoring data, chemical species including OA, NO_3^-, SO_4^{2-}, NH_4^+, Cl^-, and BC were all selected to input HERM model for three pilot cities. For inorganic elements, Si, K, Ca, Cr, Mn, Fe, Ni, Cu, Zn, As, Se, Ba, and Pb in Xi'an and Beijing, and Si, K, Ca, Ti, Cr, Mn, Fe, Ni, Cu, Zn, As, Se, Ba, and Pb in Shijiazhuang were selected for source apportionment, respectively.

The uncertainty data of chemical species inputting HERM was calculated according to the recommendation in the PMF5.0 user guideline. If the measured chemical species concentration is greater than the minimum detection limit (MDL) provided, the uncertainty (Unc) calculation is based following equation:

$$Unc_i = \sqrt{(C_i \times E_i)^2 + (0.5 \times MDL_i)^2} \tag{1}$$

where C_i represents measured concertation for species i, E_i represents error fraction of species i. For online measured data, the error fraction was recommended to use 10% (Rai et al., 2020). If the measured concentration is less than or equal to the MDL provided, the Unc is calculated as the following equation:

$$Unc = \frac{5}{6} \times MDL \tag{2}$$

Text S2 Diagnostics of HERM solutions

In this study, factors numbering from two to ten were selected and run in the HERM software. Each factor solution was run thirty times with completely unconstrained profiles to explore the possible sources. The optimal factor number solution was determined by examining the ratio of Q and expected Q (Q_{exp}). The Q_{exp} in HERM was equal to (samples ×species – factors × (samples + species) + the number of constrained source profiles). As shown in Fig. S5, the value of Q/Q_{exp} decreased with the increase of the factor number, which suggests increasing the factor number could lead to a better explanation of the variance by HERM. However, the utility of increasing factors declined with the number of factors. Too many factors could cause splitting profiles, although the Q/Q_{exp} may be desirable (Liu et al., 2021; Salameh et al., 2018, 2016). Thus, the drops of Q/Q_{exp} ($\Delta Q/Q_{exp}$) were subsequently evaluated to choose the optimal solution factor number. As shown in Table S2, when the number of factors increases to more than six in Xi'an, the value of $\Delta Q/Q_{exp}$ shows a relatively stable change trend. A six-factor solution is preferable because $\Delta Q/Q_{exp}$ between the five-solution and six-solution is smaller than that between the six-solution and seven-solution (Liu et al., 2021). In addition, secondary nitrate plus sulfate and biomass burning were mixed when the factor number was five, and vehicle emission was split into two profiles when the factor number was seven

44   (Table S3). Therefore, the six-factor solution was determined as the optimal HERM solution for Xi'an. Similar

45   criterias were used for Shijiazhuang and Beijing, six-factor and eight-factor solutions were determined as optimal

46   HERM solutions, respectively.
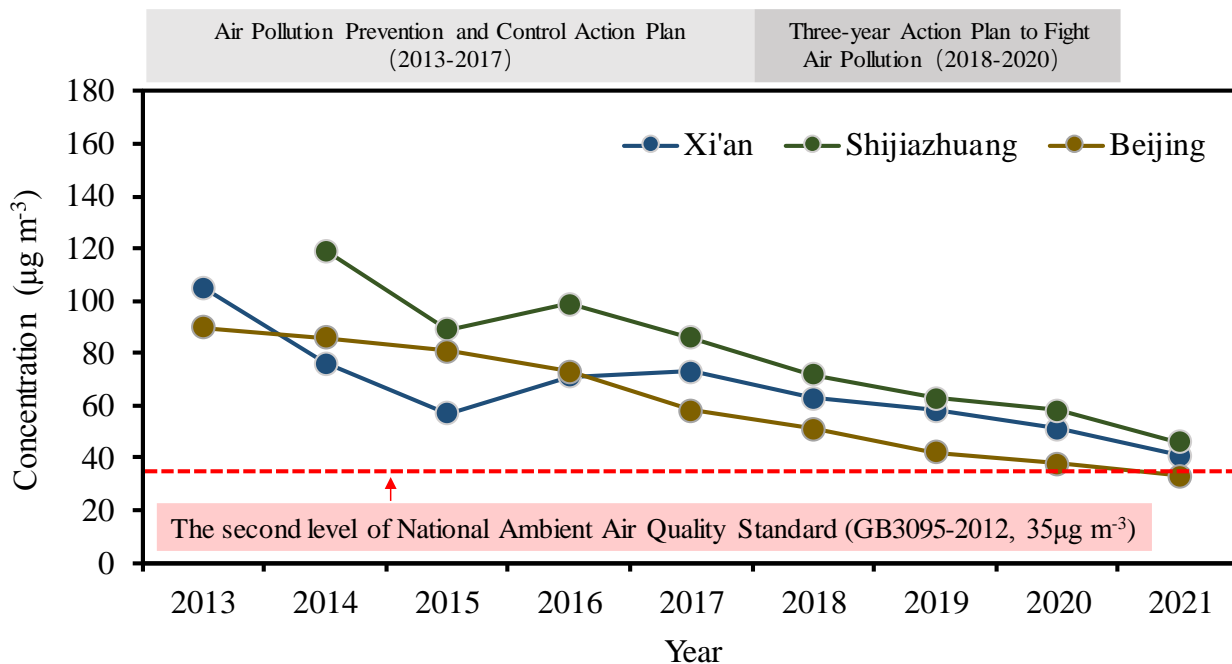
Figure S1. Annual average concentration of $PM_{2.5}$ from 2013 to 2021 in Xi'an, Shijiazhuang, and Beijing. (The data are from the website of the local Ecological Environment Bureau, Xi'an: http://xaepb.xa.gov.cn/, Shijiazhuang: https://sthjj.sjz.gov.cn/, Beijing: http://sthjj.beijing.gov.cn/). The red dotted line represents the second level of the National Ambient Air Quality Standard (GB3095-2012, 35 μg m^{-3})
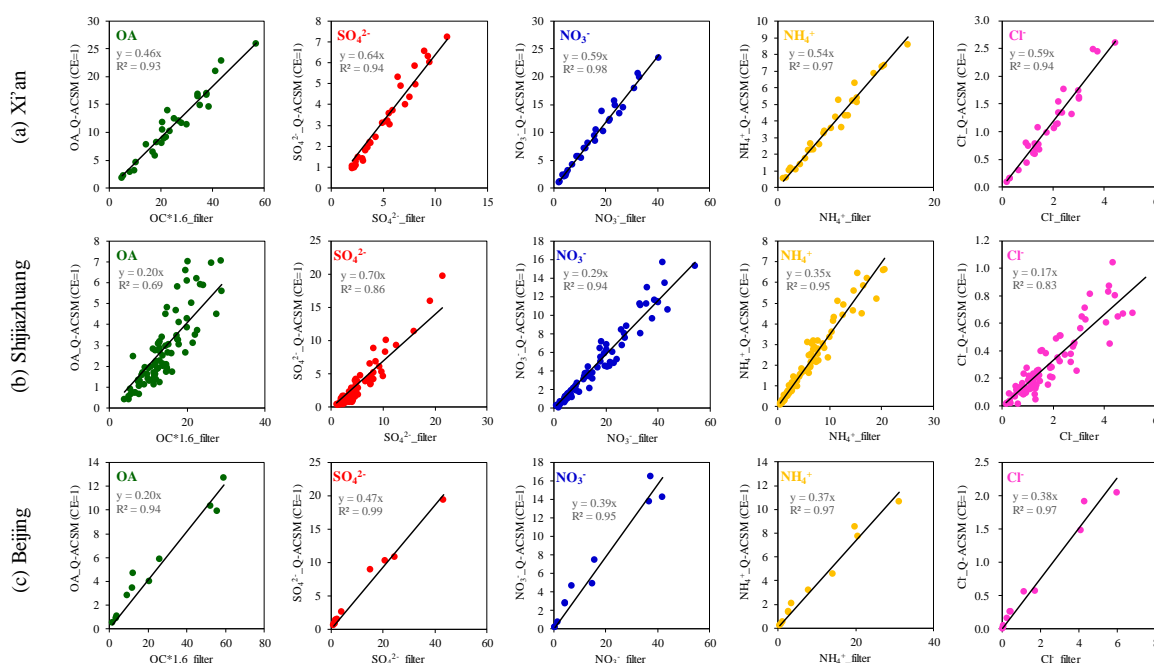
Figure S2. Correction of chemical components measured by Q-ACSM in different cities. During the campaigns, offline filter samples were simultaneously sampled for the correction. In summary, 29 offline samples in Xi'an, 83 offline samples in Shijiazhuang, and 10 offline samples in Beijing were sampled respectively.

57
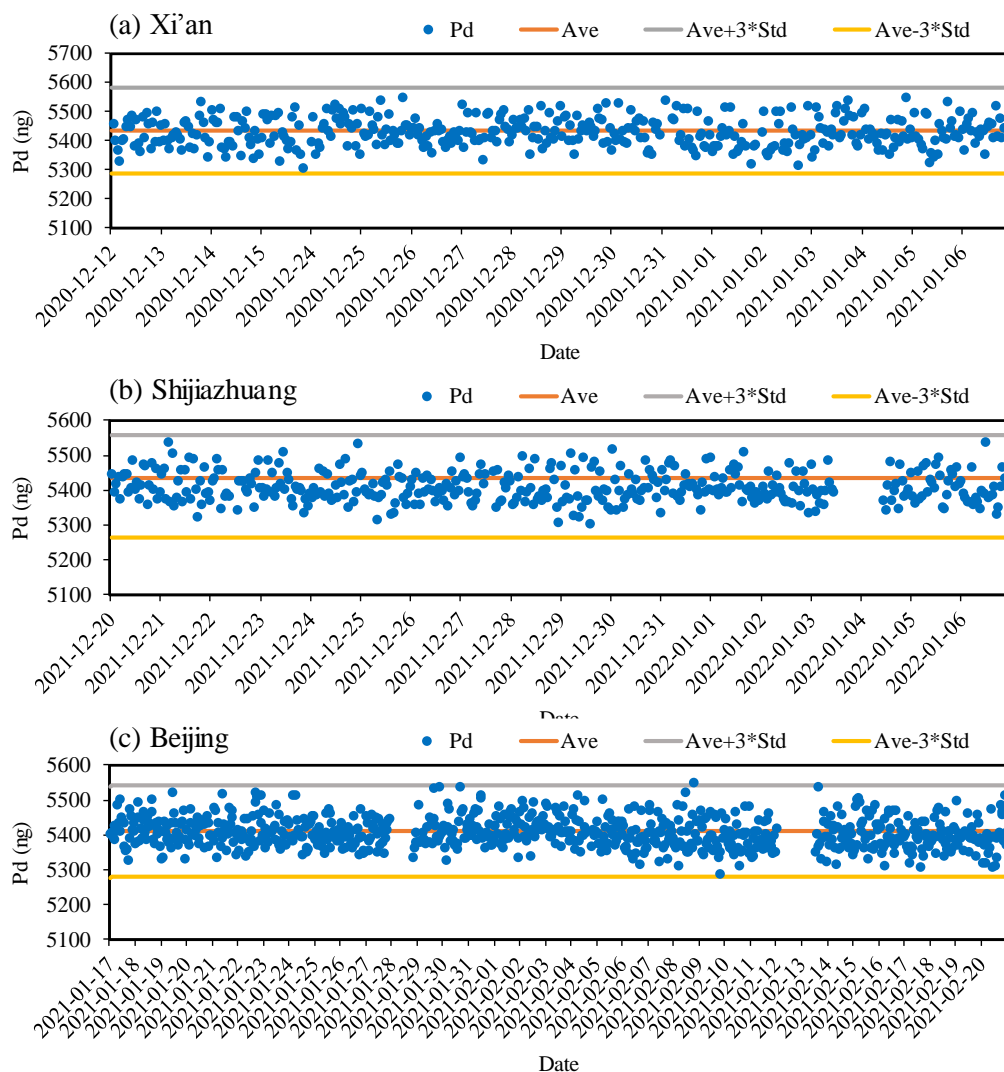
Figure S3. Concentration of the internal standard element (Pd) of Xact625 during sampling periods in (a) Xi'an, (b) Shijiazhuang, and (c) Beijing.

60
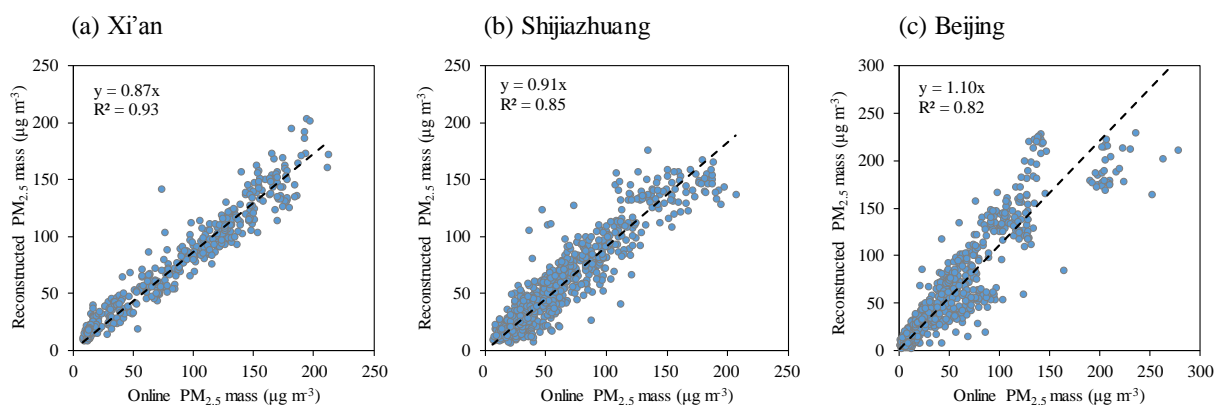
Figure S4. Correlation of online and reconstructed PM$_{2.5}$ concentration in (a) Xi'an, (b) Shijiazhuang, and (c) Beijing during the campaigns. The online PM$_{2.5}$ mass data in the X axis from national monitor stations near sampling sites.
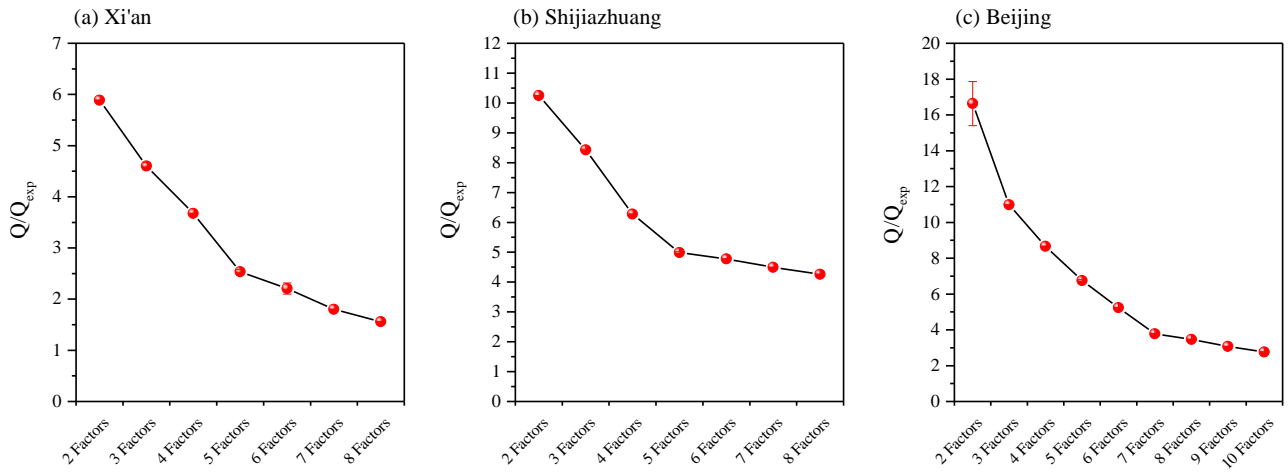
Figure S5. Values of Q/Q$_{exp}$ for the unconstrained profile solutions with two to ten factors based on thirty runs in (a) Xi'an, (b) Shijiazhuang, and (c) Beijing, respectively.
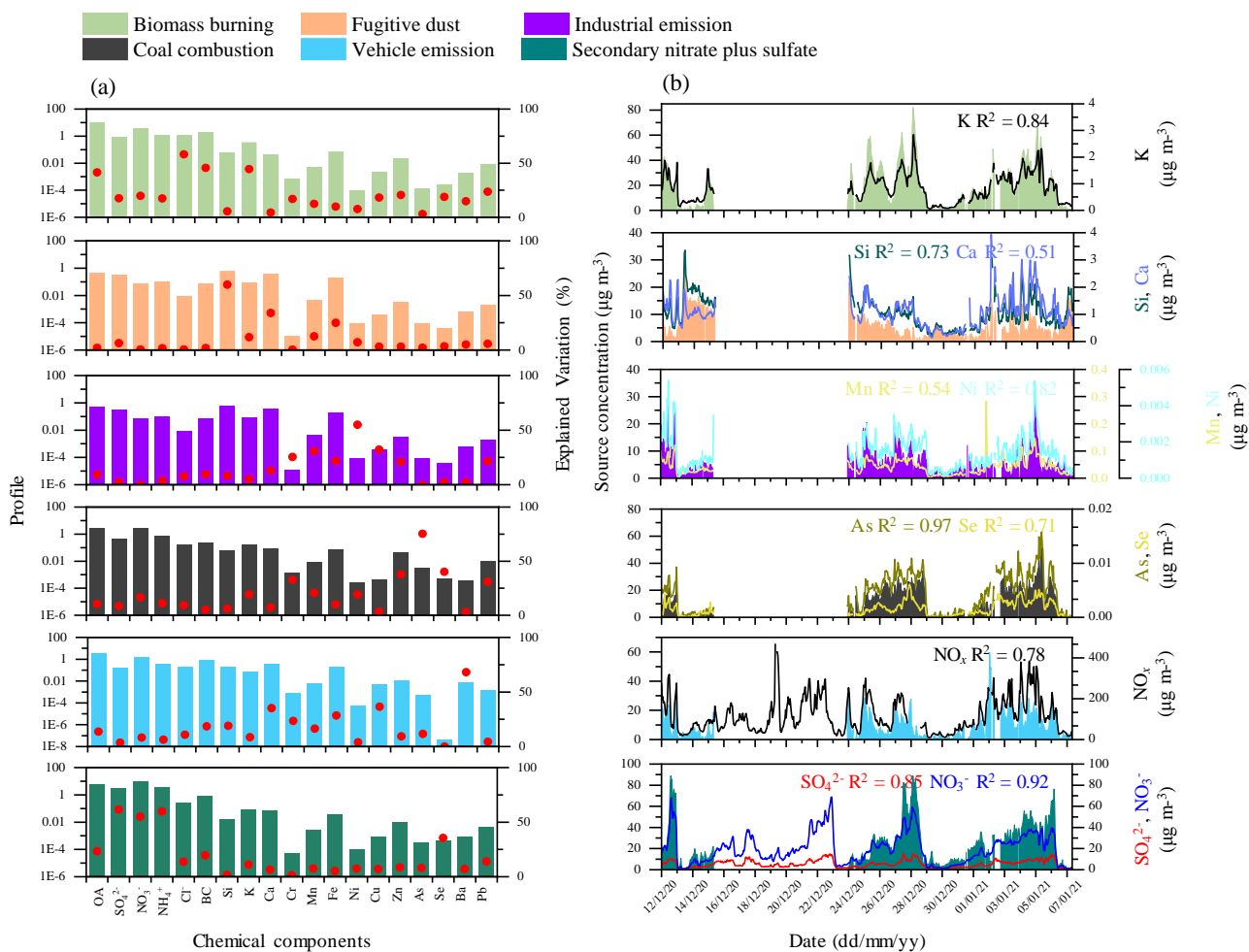
Figure S6. (a) Sources profiles obtained from HERM with a six-factor solution in Xi'an, the columns in each factor are the profile that displays the relative relation of the absolute values of variables. The red dot represents the explained variation (EV) in species for different factors. (b) Time series plots of sources concentration, including biomass burning, fugitive dust, industrial emission, coal combustion, vehicle emission, and secondary nitrate plus sulfate. The corresponding time trends of chemical tracers are also shown.

72
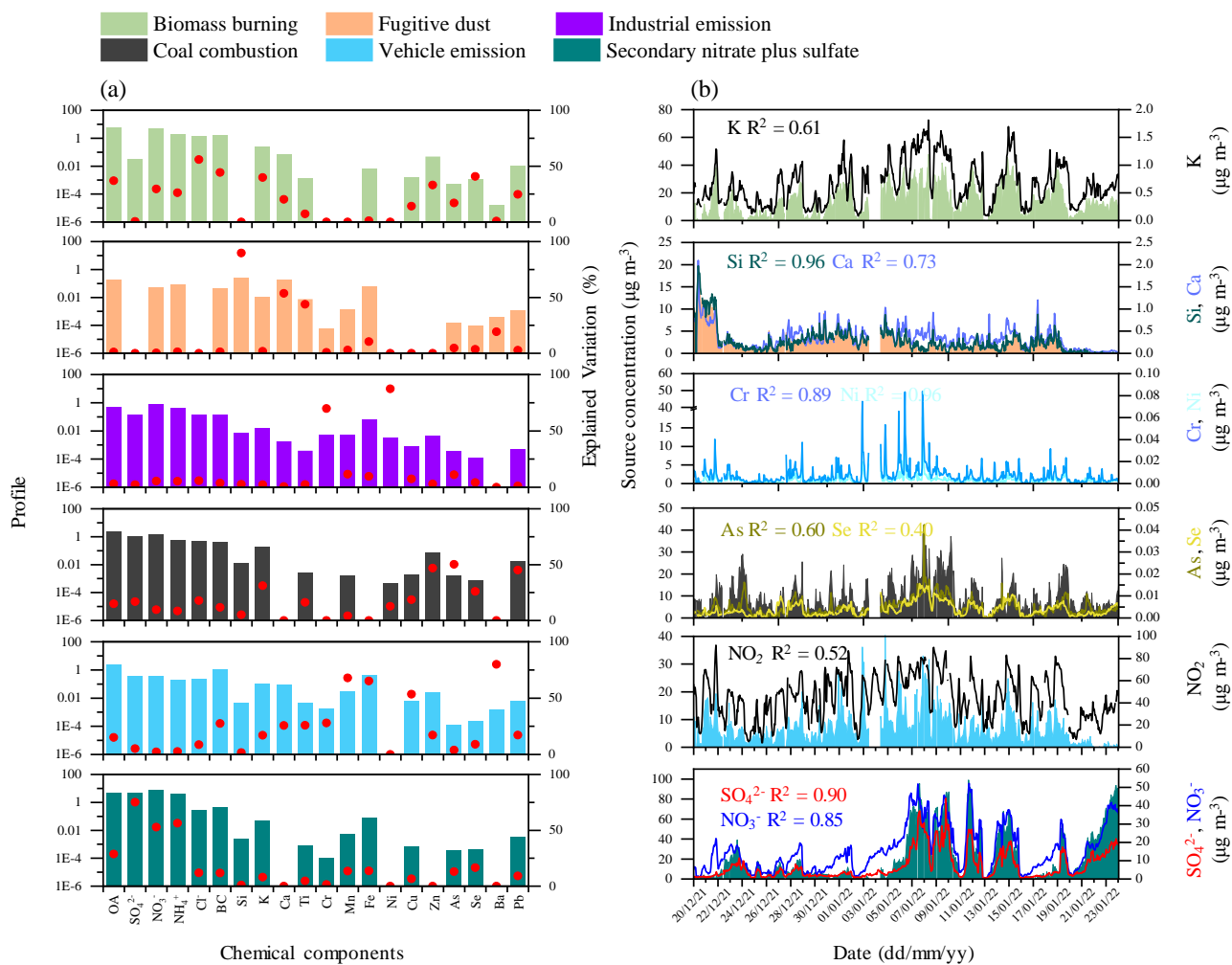
Figure S7. (a) Sources profiles obtained from HERM with a six-factor solution in Shijiazhuang, the columns in each
factor are the profile that displays the relative relation of the absolute values of variables. The red dot represents the
explained variation (EV) in species for different factors. (b) Time series plots of sources concentration, including
biomass burning, fugitive dust, industrial emission, coal combustion, vehicle emission, and secondary nitrate plus
sulfate. The corresponding time trends of chemical tracers are also shown.
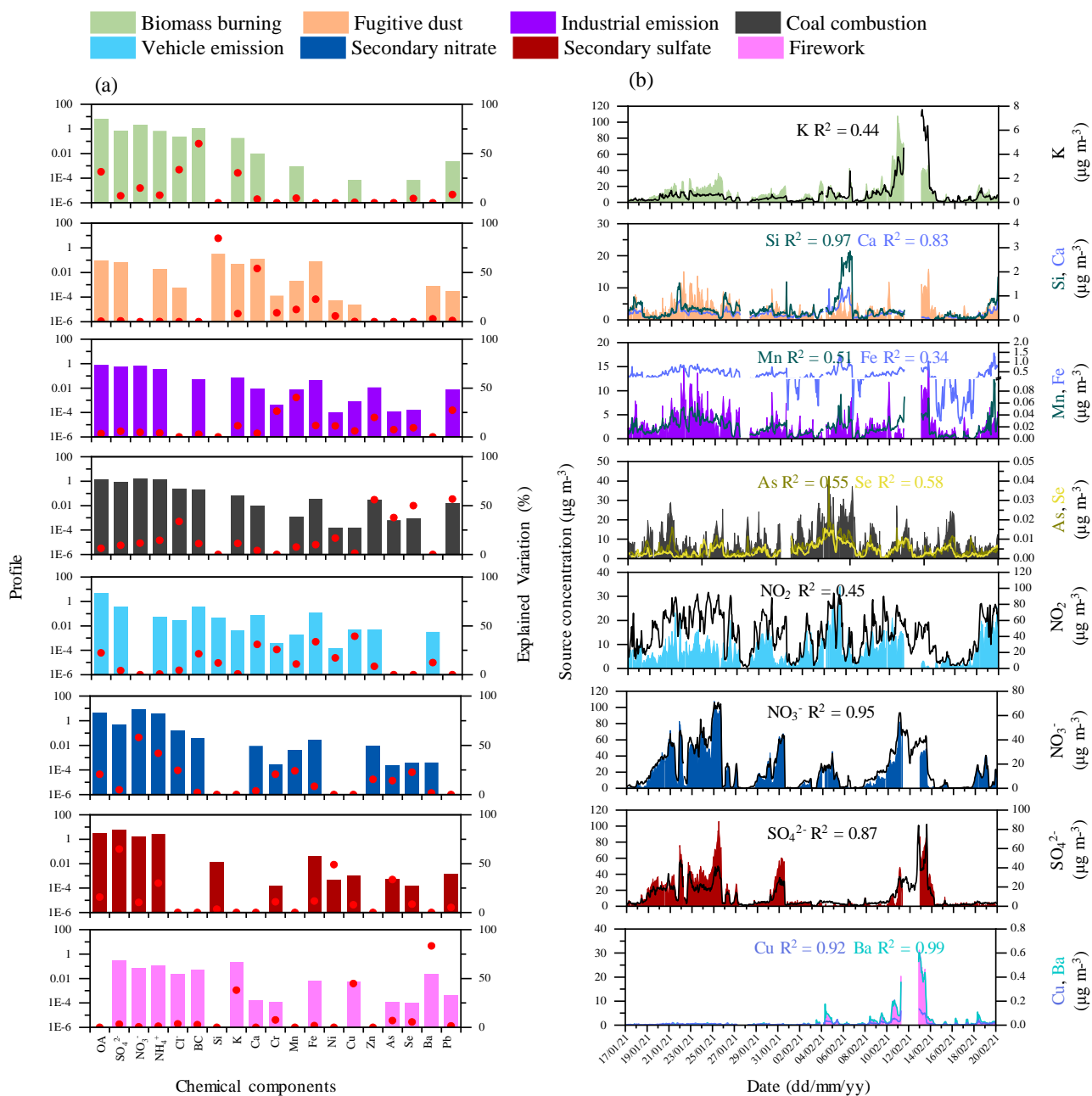
78
79 **Figure S8.** (a) Sources profiles obtained from HERM with an eight-factor solution in Beijing, the columns in each
80 factor are the profile that displays the relative relation of the absolute values of variables. The red dot represents the
81 explained variation (EV) in species for different factors. (b) Time series plots of sources concentration, including
82 biomass burning, fugitive dust, industrial emission, coal combustion, vehicle emission, secondary nitrate, secondary
83 sulfate, and firework. The corresponding time trends of chemical tracers are also shown.

84

(a) Xi'an   (b) Shijiazhuang   (c) Beijing

85
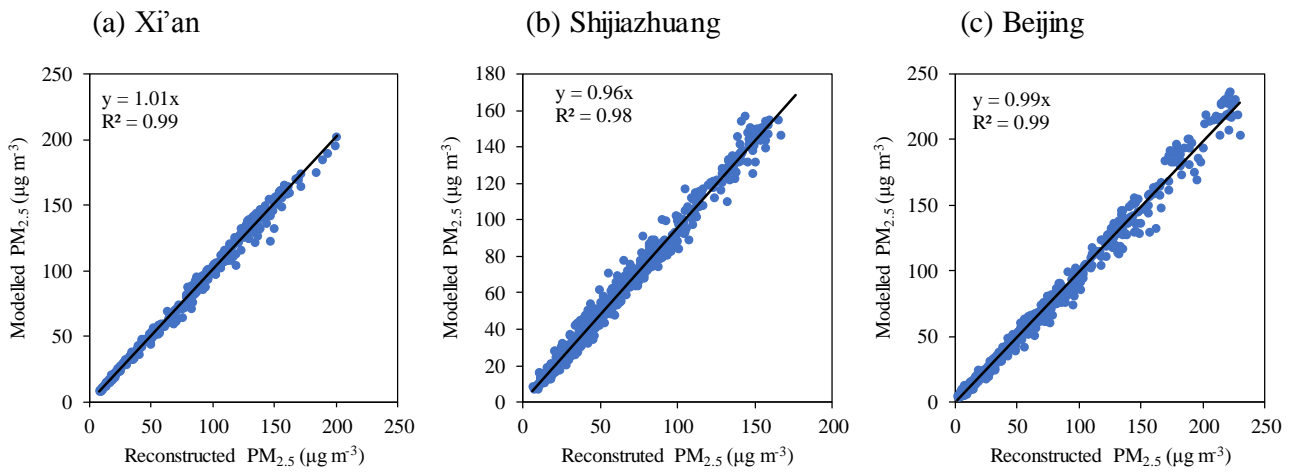
Figure S9. Correlation between reconstructed $PM_{2.5}$ and modeled $PM_{2.5}$ mass concentrations derived by HERM in Xi'an, Shijiahuznag, and Beijing with optimal solutions

88

89
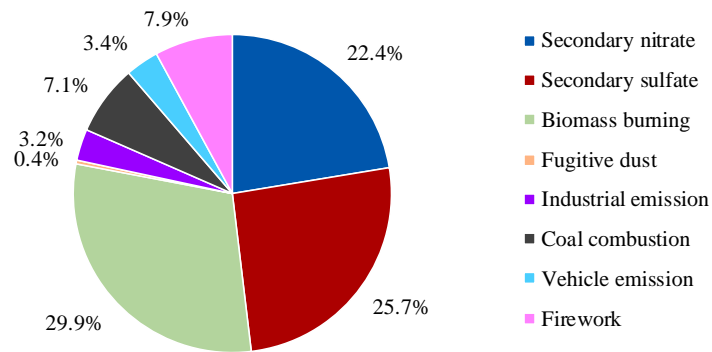
Figure S10. Source contribution of $PM_{2.5}$ during Chinese Spring Festival (from New Year's Eve to January 3rd of the Lunar Calendar) in Beijing

92
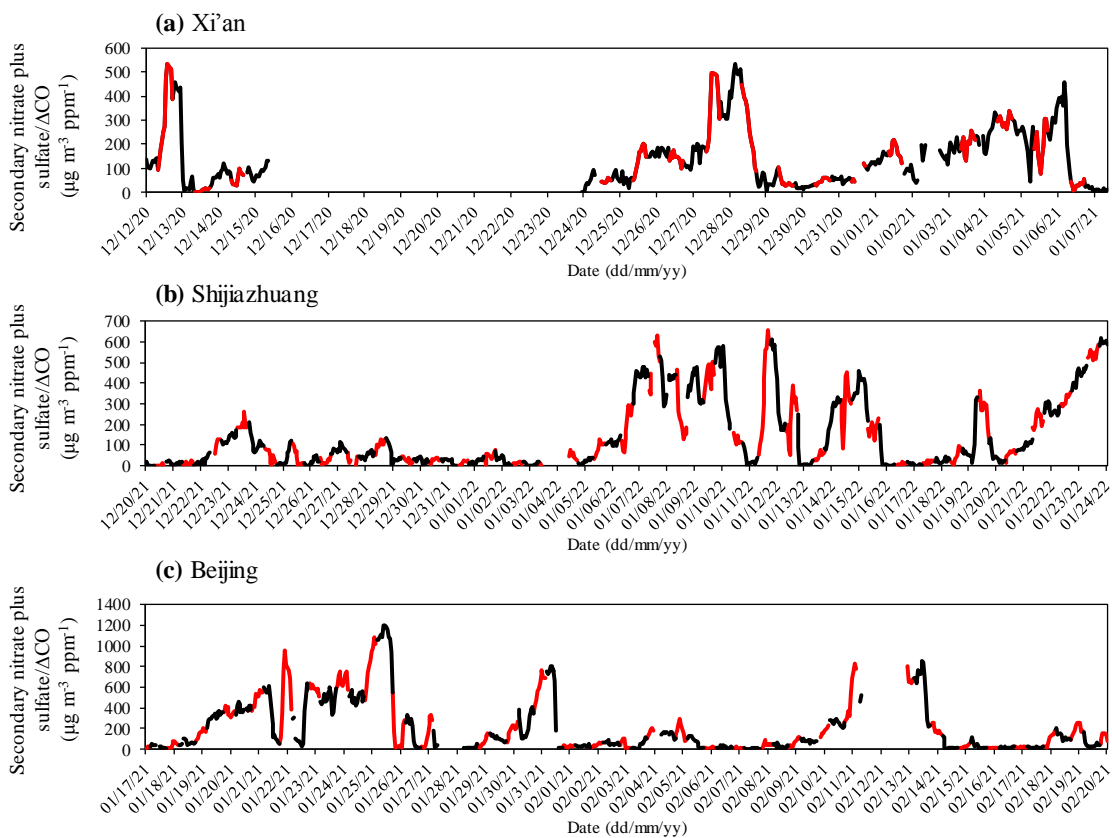
Figure S11. Time series plots of secondary nitrate plus sulfate/ΔCO in (a) Xi'an, (b) Shijiazhuang, and (c) Beijing. The red and black lines represent daytime (08:00-17:00 LST) and nighttime (18:00 - 07:00 the next day LST), respectively.

96

97
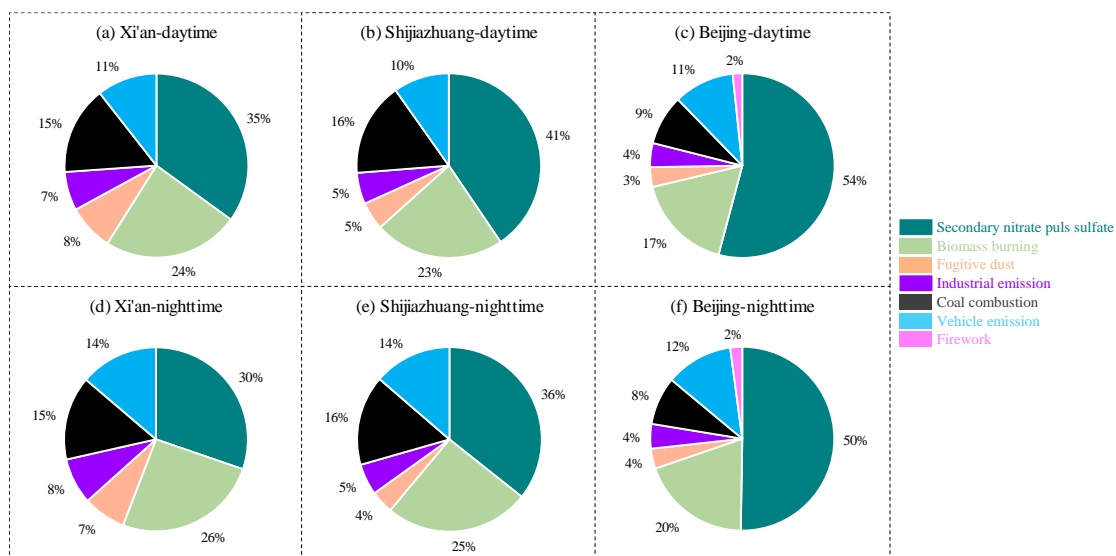
Figure S12. Source contribution of $PM_{2.5}$ in three pilot cities during daytime and nighttime, respectively.

99
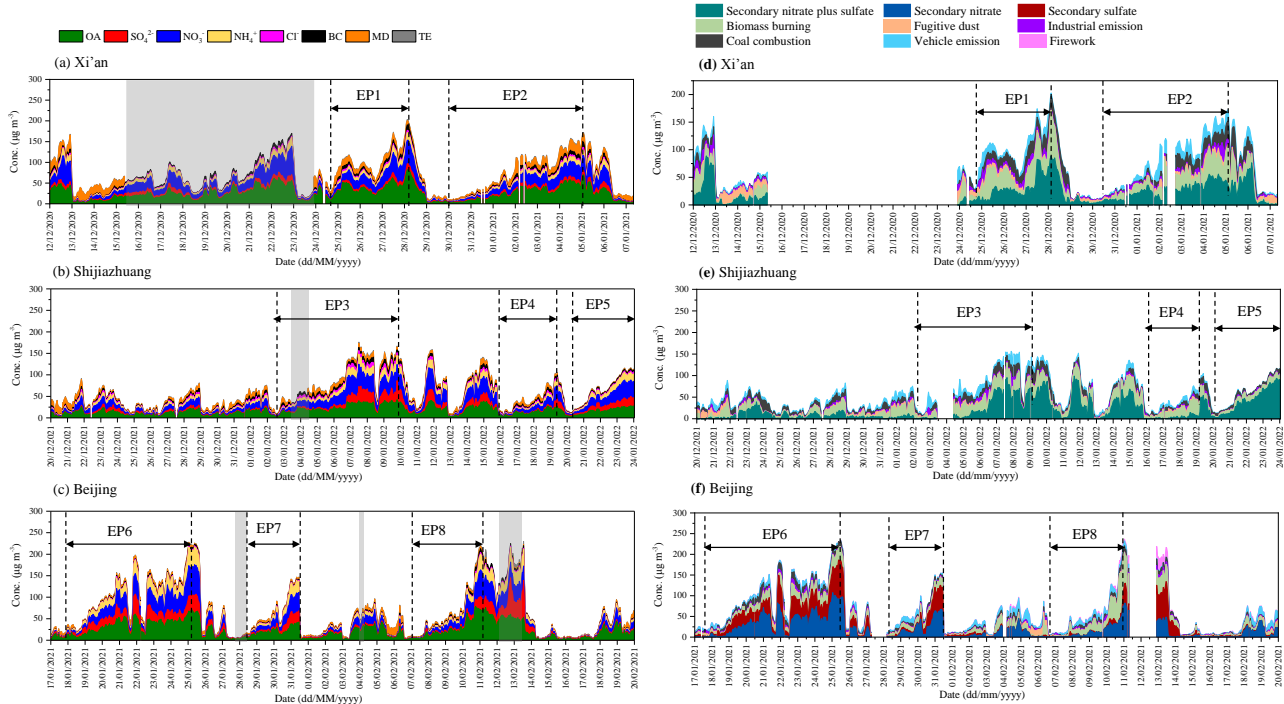
Figure S13. The pollution episodes selection according to temporal variation of PM$_{2.5}$ chemical components (a-c) and source contribution (d-f) during the campaigns in Xi'an, Shijiazhuang, and Beijing, respectively. The gray shape parts were lack of MD values due to the out-of-order Xact625, and missing values in the time series owing to the out-of-order ACSM, AE33, and Xact625 at the same time.

104
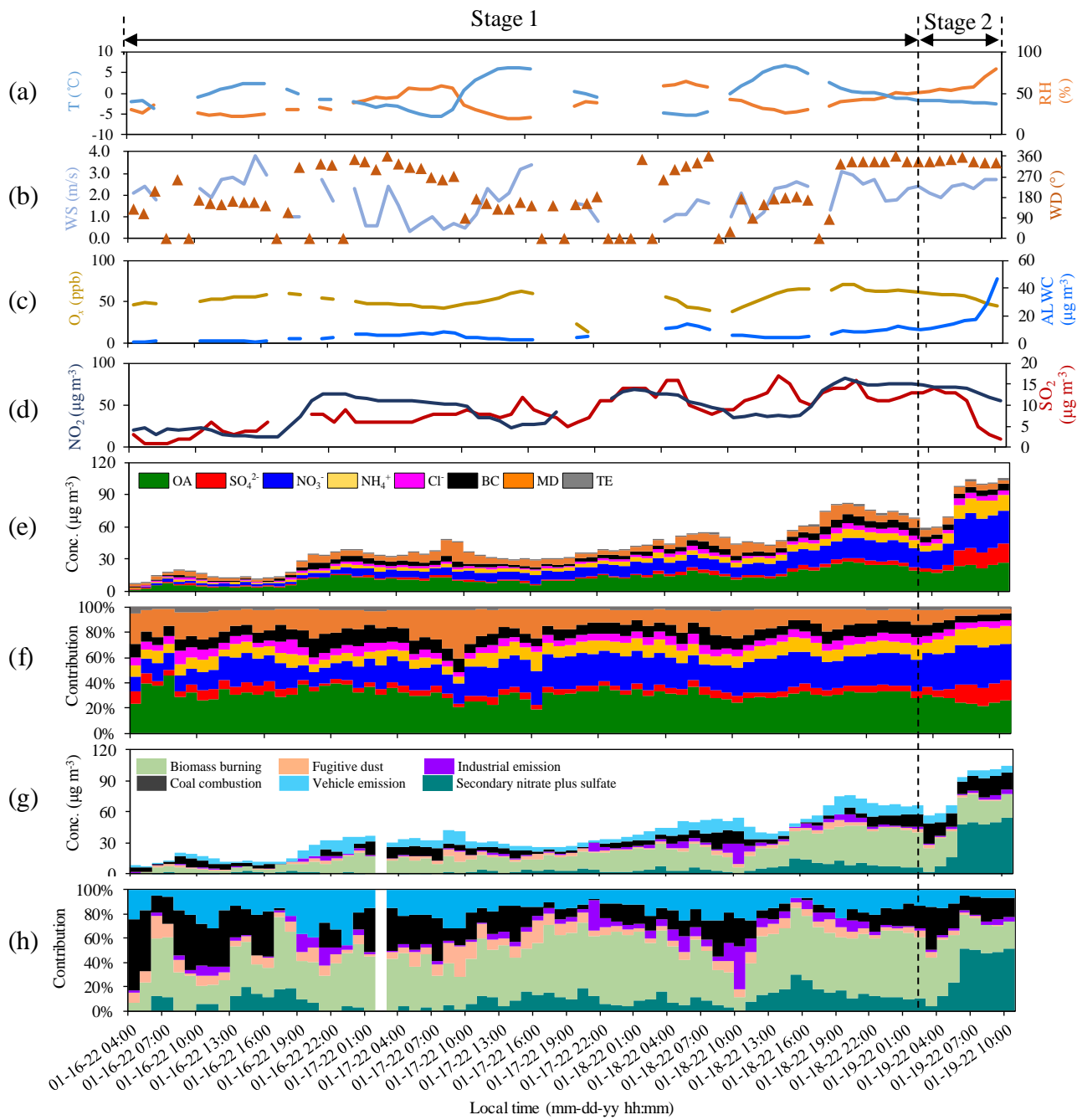
Figure S14. Time series of T and RH (a), WS and WD (b), O_x and ALWC (c), NO_2 and SO_2 (d), chemical components (e,f), and source contribution (g, h) of $PM_{2.5}$ during EP4 in Shijiazhuang.

107

108
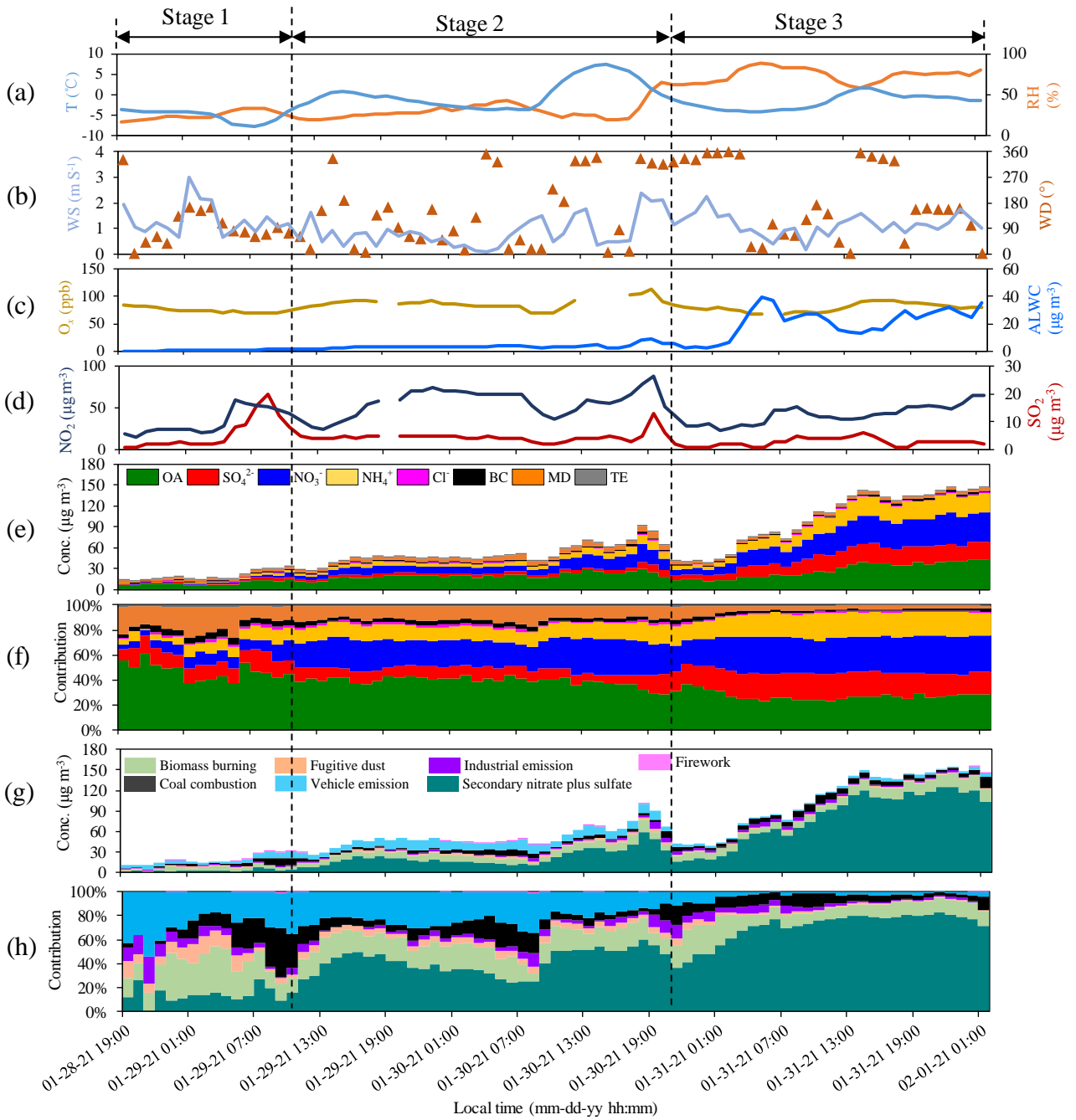
Figure S15. Time series of T and RH (a), WS and WD (b), O_x and ALWC (c), NO_2 and SO_2 (d), chemical components (e, f), and source contribution (g, h) of $PM_{2.5}$ during EP7 in Beijing

111

112
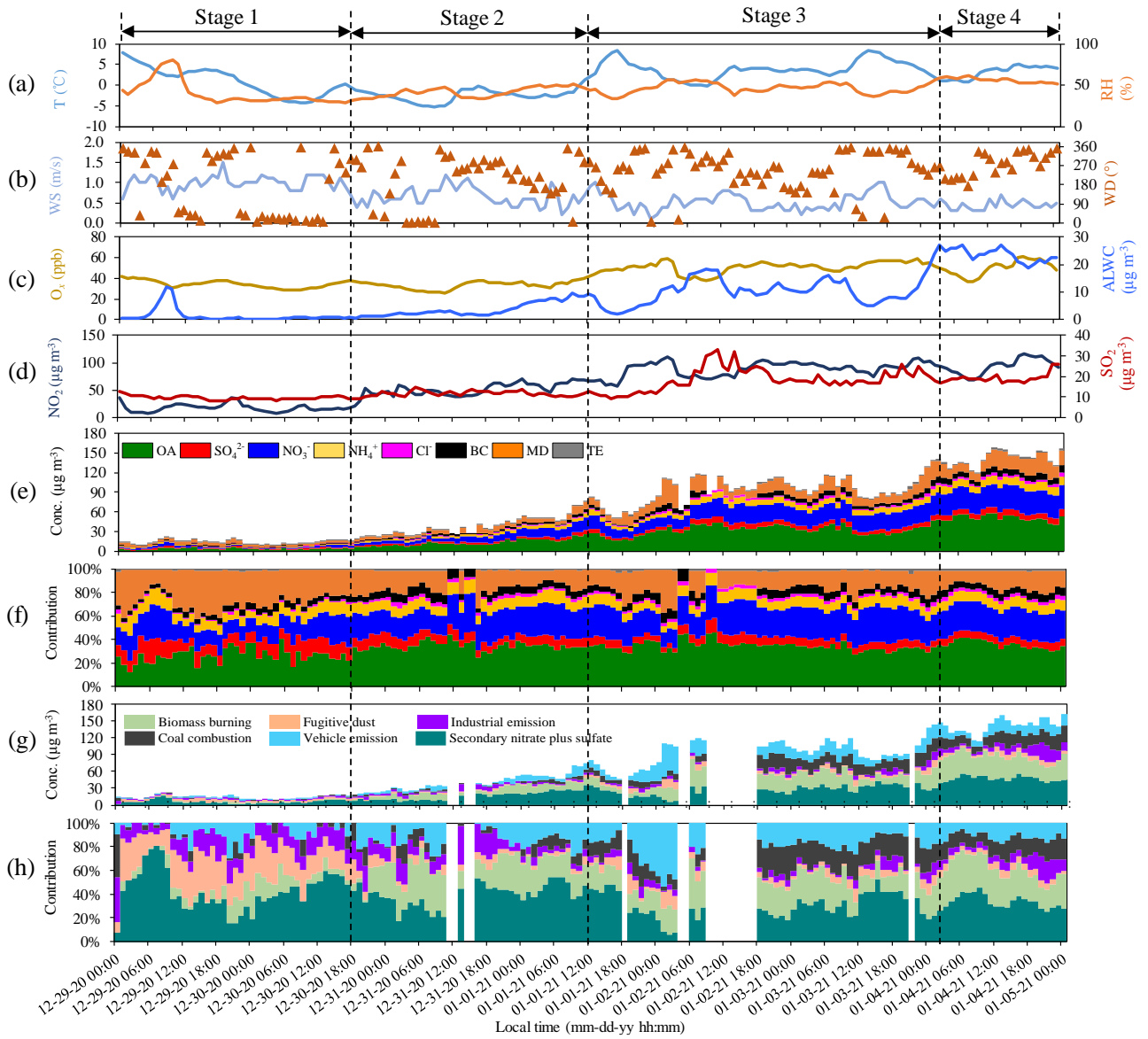
Figure S16. Time series of T and RH (a), WS and WD (b), O_x and ALWC (c), NO_2 and SO_2 (d), chemical components (e, f), and source contribution (g, h) of $PM_{2.5}$ during EP2 in Xi'an.

115   **Table S1.** Detailed information on complementary data for sampling sites

Sampling site	National Air Quality Monitoring Station	National Meteorological Station	complementary data
Xi'an	Gaoxinxiqu station, 1.1km from the sampling site	Haidian station, 7.6 km from the sampling site	hourly $PM_{2.5}$, NO_x, NO_2, CO, SO_2, O_3, WS, WD, T, RH
Shijiazhuang	Gaoxinqu station, 4.2 km from the sampling site	Shijiazhuang station, 23.8 km from the sampling site	hourly $PM_{2.5}$, NO_2, CO, SO_2, O_3, WS, WD, T, RH
Beijing	ChaoyangAotizhongxin station, 1.2 km from the sampling site	Jinghe station, 21.2 km from the sampling site	hourly $PM_{2.5}$, NO_2, CO, SO_2, O_3, WS, WD, T, RH

116   Note: WS: wind speed, WD: wind direction, T: temperature, RH: relative humidity.

117

118   **Table S2.** The $\Delta Q/Q_{exp}$[a] value with increasing factor number from two to ten of the runs in Xi'an, Shijiazhuang, and
119   Beijing.

Parameter[b]	$\Delta Q/Q_{exp}$		
	Xi'an	Shijiazhuang	Beijing
F2-F3	1.3	1.8	5.7
F3-F4	0.9	2.2	2.3
F4-F5	1.1	1.2	1.9
F5-F6	0.4	0.3	1.5
F6-F7	0.3	0.3	1.5
F7-F8	0.2	0.2	0.3
F8-F9			0.4
F9-F10			0.3

120   [a] $\Delta Q/Q_{exp}$ means the difference of Q/Q_{exp} of two sequent factor numbers.

121   [b] Parameters represent the factor numbers (F) – (F+1).

122

123 **Table S3.** Sources diagnostics with increasing factor numbers from four to ten of the runs in Xi'an, Shijiazhuang,
124 and Beijing.

Factor number	Sources identification		
	Xi'an	Shijiazhuang	Beijing
4	Secondary nitrate plus sulfate mixed with biomass burning and coal burning mixed with industrial emission	i) Secondary nitrate plus sulfate mixed with primary sources including biomass burning and coal combustion ii) Biomass burning, coal combustion, and vehicle emission was also mixed	i) Secondary sources mixed with primary sources including biomass burning, coal combustion, and vehicle emission ii) Biomass burning and coal combustion was mixed
5	Secondary nitrate plus sulfate mixed with biomass burning	Biomass burning, coal combustion, and vehicle emissions were mixed	Secondary sulfate mixed with coal combustion and industrial emission; secondary nitrate mixed with biomass burning
6	Six individual sources were identified	Six individual sources were identified	Secondary sulfate mixed with coal combustion and secondary nitrate mixed with industrial emission
7	Vehicle emission was split into two profiles	Coal combustion was split into two profiles	Secondary sulfate mixed with coal combustion
8	Vehicle emission and industrial emission was split into two profiles, respectively.	Vehicle emission and coal combustion were split into two profiles, respectively.	Eight individual sources were identified
9			Coal combustion was split into two profiles
10			Coal combustion and biomass burning were split into two profiles, respectively.

125

126 **Table S4.** Average concentrations of reconstructed PM$_{2.5}$ and its chemical species in Xi'an, Shijiazhuang, and Beijing
127 during the campaign* (μg m^{-3})

Chemical Species	Xi'an	Shijiazhuang	Beijing
Reconstructed PM$_{2.5}$	77 ± 47	60 ± 39	64 ± 57
OA	25.9 ± 18.0	16.0 ± 9.7	22.1 ± 18.1
SO$_4^{2-}$	5.2 ± 3.4	7.0 ± 7.6	9.6 ± 11.3
NO$_3^-$	18.5 ± 14.5	15.8 ± 12.5	15.2 ± 16.7
NH$_4^+$	6.2 ± 4.5	7.0 ± 5.5	9.2 ± 10.3
Cl$^-$	1.9 ± 1.5	2.8 ± 2.2	0.7 ± 0.8
BC	4.5 ± 3.2	3.9 ± 2.5	1.9 ± 1.8
MD[a]	13.2 ± 7.0	6.0 ± 4.0	4.8 ± 3.8
TE[b]	1.1 ± 0.7	1.0 ± 0.6	0.9 ± 1.5

128 * Data during Xact625 failure shown in Figure S2 was excluded to calculate average concentration of campaign

129 [a] MD means mineral dust, which is equal to 2.20Al + 2.49Si + 1.63Ca + 2.42Fe + 1.94Ti

130 [b] TE means trace elements which is equal to K + Cr + Mn + Ni + Cu + Zn + As +Se + Ba + Pb

131

132 **Table S5.** The nitrogen oxidation ratio (NOR) and sulfur oxidation ratio (SOR) in Xi'an, Beijing, and Shijiazhuang
133 during the campaigns[a]

Parameters	Xi'an	Shijiazhuang	Beijing
NOR	0.15 ± 0.08	0.20 ± 0.11	0.16 ± 0.12
SOR	0.18 ± 0.08	0.36 ± 0.25	0.48 ± 0.23

134 [a] NOR = n(NO$_3^-$)/(n(NO$_3^-$) + n(NO$_2$)); SOR = n(SO$_4^{2-}$)/(n(SO$_4^{2-}$) + n(SO$_2$)). where n(NO$_3^-$), n(NO$_2$), n(SO$_4^{2-}$), and n(SO$_2$) are the molar
135 concentrations of NO$_3^-$, NO$_2$, SO$_4^{2-}$, and SO$_2$, respectively.

136

137 **Table S6.** The concentration of PM$_{2.5}$ and its main chemical components during wintertime in Xi'an, Shijiazhuang,
138 and Beijing in the last decades.

City	Year	PM$_{2.5}$	OA[a]	EC	SO$_4^{2-}$	NO$_3^-$	NH$_4^+$	Others	References
		μg m^{-3}	μg m^{-3}	μg m^{-3}	μg m^{-3}	μg m^{-3}	μg m^{-3}	μg m^{-3}	
	2003	356	153.3	21.5	53.8	29.2	29.6	68.9	Cao et al., 2012
	2006	230	57.4	11.4	45.9	20.6	14.2	80.0	Xu et al., 2016
	2008	199	48.3	9.9	42.5	20.8	11.0	66.9	Xu et al., 2016
	2010	233	60.0	14.7	30.6	22.9	12.3	92.8	Xu et al., 2016
Xi'an	2012	196	56.3	8.2	27.0	19.2	13.3	71.9	Zhang et al., 2015
	2013	263	45.8	7.1	31.7	29.2	17.1	132.5	Niu et al., 2016
	2014	156	57.4	2.5	16.2	20.6	9.4	49.7	Dai et al., 2018
	2018	189	42.1	4.9	9.7	14.5	6.6	111.0	Wang et al., 2022
	2020*	77	25.9	4.5	5.2	18.5	6.2	16.2	This study
	2010	227	75.6	12.2	33.2	25.3	10.5	70.2	Zhao et al., 2013
	2015	232	82.0	16.3	26.6	27.4	19.8	59.7	Huang et al., 2017
Shijiazhuang	2016	193	63.2	13.5	29.5	24.0	17.0	45.8	Liu et al., 2019
	2017	97	31.2	6.5	12.5	16.5	12.5	17.8	Liu et al., 2019
	2018	96	35.8	10.1	10.5	15.3	6.3	18.0	Zhang et al., 2020
	2022*	60	16.0	3.9	7.0	15.8	7.0	9.8	This study
	2001	122	51.5	11.3	9.9	10.7	7.1	31.5	Duan et al., 2006
	2003	116	38.2	6.2	20.0	13.1	9.4	29.1	Cao et al., 2012
	2004	107	53.8	8.3	12.7	8.3	6.0	17.9	Song et al., 2007
	2010	127	42.9	7.1	14.2	17.1	5.2	40.5	Zhao et al., 2013
Beijing	2013	132	38.5	6.4	21.9	18.5	15.1	31.6	Tao et al., 2015
	2014	138	46.4	5.2	21.0	26.0	14.1	25.3	Ma et al., 2017
	2016	130	75.7	20.2	12.3	5.5	10.5	5.3	Xu et al., 2018
	2021*	64	22.1	1.9	9.6	15.2	9.2	6.4	This study

139 * study was conducted on online monitoring equipment, and the rest studies were researched on filter sampling experiments.

140 [a] Assumption of OA = 1.6 × OC for the filter-based sampling experiments

141 **Table S7.** The concentration of PM$_{2.5}$ and its source contribution during wintertime in Xi'an, Shijiazhuang, and
142 Beijing in the last decades.

City	Year	PM$_{2.5}$	Vehicle emission	Coal combustion	Secondary source	Fugitive dust	Industrial emission	Biomass burning	Others	References
		µg m^{-3}	µg m^{-3}	µg m^{-3}	µg m^{-3}	µg m^{-3}	µg m^{-3}	µg m^{-3}	µg m^{-3}	
Xi'an	2006	392	74.5	121.5	82.3	51.0	39.2	23.5		Xu et al., 2016
	2008	199	41.8	55.7	45.8	23.9	21.9	10.0		Xu et al., 2016
	2010	233	48.9	55.9	41.9	44.3	30.3	11.7		Xu et al., 2016
	2014	169	20.3	47.3	71.0	8.5	6.8	15.2		Dai et al., 2020
	2018	189	26.5	28.4		15.1	22.7	58.6	37.8	Wang et al., 2022
	2020*	77	10.0	11.6	24.6	6.2	6.2	19.3		This study
Shijiazhuang	2015	232	46.4	62.6	30.2	20.9	16.2	7.0	48.7	Huang et al., 2017
	2016	181	23.5	54.3	54.3	30.8	9.1		7.2	Liu et al., 2018
	2019	119	21.4	21.4	42.8	21.4	6.0	6.0		Diao et al., 2021
	2022*	60	7.2	9.6	22.8	2.4	3.0	14.4		This study
Beijing	2004	107	8.6	40.7	19.3	7.5		16.1	15.0	Song et al., 2007
	2010	139		79.2	8.3	22.2	16.7	9.7	2.8	Zhang et al., 2013
	2013	159	9.5	41.3	79.5	15.9		9.5	3.2	Huang et al., 2014
	2015	125	48.8	15.0	23.8	8.8	2.5	6.3	18.8	Huang et al., 2017
	2021*	64	7.0	5.8	33.3	2.6	2.6	11.5	1.3	This study

143 * study was conducted on online monitoring equipment, and the rest studies were researched on filter sampling experiments.
144

References:

Cao, J.-J., Shen, Z.-X., Chow, J. C., Watson, J. G., Lee, S.-C., Tie, X.-X., Ho, K.-F., Wang, G.-H., and Han, Y.-M.: Winter and summer $PM_{2.5}$ chemical compositions in fourteen Chinese cities, J. Air Waste Manage., 62, 1214–1226, https://doi.org/10.1080/10962247.2012.701193, 2012.

Dai, Q., Bi, X., Liu, B., Li, L., Ding, J., Song, W., Bi, S., Schulze, B. C., Song, C., Wu, J., Zhang, Y., Feng, Y., and Hopke, P. K.: Chemical nature of $PM_{2.5}$ and PM_{10} in Xi'an, China: Insights into primary emissions and secondary particle formation, Environ. Pollut., 240, 155–166, https://doi.org/10.1016/j.envpol.2018.04.111, 2018.

Dai, Q., Hopke, P. K., Bi, X., and Feng, Y.: Improving apportionment of $PM_{2.5}$ using multisite PMF by constraining G-values with a prioriinformation, Sci. Total Environ., 736, 139657, https://doi.org/10.1016/j.scitotenv.2020.139657, 2020.

Diao, L., Zhang, H., Liu, B., Dai, C., Zhang, Y., Dai, Q., Bi, X., Zhang, L., Song, C., and Feng, Y.: Health risks of inhaled selected toxic elements during the haze episodes in Shijiazhuang, China: Insight into critical risk sources, Environ. Pollut., 276, 116664, https://doi.org/10.1016/j.envpol.2021.116664, 2021.

Duan, F., He, K., Ma, Y., Yang, F., Yu, X., Cadle, S., Chan, T., and Mulawa, P.: Concentration and chemical characteristics of $PM_{2.5}$ in Beijing, China: 2001–2002, Sci. Total Environ., 355, 264–275, https://doi.org/10.1016/j.scitotenv.2005.03.001, 2006.

Huang, R.-J., Zhang, Y., Bozzetti, C., Ho, K.-F., Cao, J.-J., Han, Y., Daellenbach, K. R., Slowik, J. G., Platt, S. M., Canonaco, F., Zotter, P., Wolf, R., Pieber, S. M., Bruns, E. A., Crippa, M., Ciarelli, G., Piazzalunga, A., Schwikowski, M., Abbaszade, G., Schnelle-Kreis, J., Zimmermann, R., An, Z., Szidat, S., Baltensperger, U., Haddad, I. E., and Prévôt, A. S. H.: High secondary aerosol contribution to particulate pollution during haze events in China, Nature, 514, 218–222, https://doi.org/10.1038/nature13774, 2014.

Huang, X., Liu, Z., Liu, J., Hu, B., Wen, T., Tang, G., Zhang, J., Wu, F., Ji, D., Wang, L., and Wang, Y.: Chemical characterization and source identification of $PM_{2.5}$ at multiple sites in the Beijing–Tianjin–Hebei region, China, Atmos. Chem. Phys., 17, 12941–12962, https://doi.org/10.5194/acp-17-12941-2017, 2017.

Liu, B., Cheng, Y., Zhou, M., Liang, D., Dai, Q., Wang, L., Jin, W., Zhang, L., Ren, Y., Zhou, J., Dai, C., Xu, J., Wang, J., Feng, Y., and Zhang, Y.: Effectiveness evaluation of temporary emission control action in 2016 in winter in Shijiazhuang, China, Atmos. Chem. Phys., 18, 7019–7039, https://doi.org/10.5194/acp-18-7019-2018, 2018.

Liu, G., Xin, J., Wang, X., Si, R., Ma, Y., Wen, T., Zhao, L., Zhao, D., Wang, Y., and Gao, W.: Impact of the coal banning zone on visibility in the Beijing-Tianjin-Hebei region, Sci. Total Environ., 692, 402–410, https://doi.org/10.1016/j.scitotenv.2019.07.006, 2019.

Liu, H., Wang, Q., Ye, J., Su, X. li, Zhang, T., Zhang, Y., Tian, J., Dong, Y., Chen, Y., Zhu, C., Han, Y., and Cao, J.: Changes in Source‑Specific Black Carbon Aerosol and the Induced Radiative Effects Due to the COVID‑19 Lockdown, Geophys. Res. Lett., 48, https://doi.org/10.1029/2021GL092987, 2021.

178   Ma, Q., Wu, Y., Tao, J., Xia, Y., Liu, X., Zhang, D., Han, Z., Zhang, X., and Zhang, R.: Variations of Chemical Composition
179   and Source Apportionment of $PM_{2.5}$ during Winter Haze Episodes in Beijing, Aerosol Air Qual. Res., 17, 2791–2803,
180   https://doi.org/10.4209/aaqr.2017.10.0366, 2017.

181   Niu, X., Cao, J., Shen, Z., Ho, S. S. H., Tie, X., Zhao, S., Xu, H., Zhang, T., and Huang, R.: $PM_{2.5}$ from the Guanzhong
182   Plain: Chemical composition and implications for emission reductions, Atmos. Environ., 147, 458–469,
183   https://doi.org/10.1016/j.atmosenv.2016.10.029, 2016.

184   Rai, P., Furger, M., Slowik, J. G., Canonaco, F., Fröhlich, R., Hüglin, C., Minguillón, M. C., Petterson, K., Baltensperger,
185   U., and Prévôt, A. S. H.: Source apportionment of highly time-resolved elements during a firework episode from a
186   rural freeway site in Switzerland, Atmos. Chem. Phys., 20, 1657–1674, https://doi.org/10.5194/acp-20-1657-2020,
187   2020.

188   Salameh, D., Pey, J., Bozzetti, C., El Haddad, I., Detournay, A., Sylvestre, A., Canonaco, F., Armengaud, A., Piga, D.,
189   Robin, D., Prevot, A. S. H., Jaffrezo, J.-L., Wortham, H., and Marchand, N.: Sources of $PM_{2.5}$ at an urban-industrial
190   Mediterranean city, Marseille (France): Application of the ME-2 solver to inorganic and organic markers, Atmos. Res.,
191   214, 263–274, https://doi.org/10.1016/j.atmosres.2018.08.005, 2018.

192   Salameh, T., Sauvage, S., Afif, C., Borbon, A., and Locoge, N.: Source apportionment vs. emission inventories of non-
193   methane hydrocarbons (NMHC) in an urban area of the Middle East: local and global perspectives, Atmos. Chem.
194   Phys., 16, 3595–3607, https://doi.org/10.5194/acp-16-3595-2016, 2016.

195   Song, Y., Tang, X., Xie, S., Zhang, Y., Wei, Y., Zhang, M., Zeng, L., and Lu, S.: Source apportionment of $PM_{2.5}$ in Beijing
196   in 2004, J. Hazard. Mater., 146, 124–130, https://doi.org/10.1016/j.jhazmat.2006.11.058, 2007.

197   Tao, J., Zhang, L., Gao, J., Wang, H., Chai, F., and Wang, S.: Aerosol chemical composition and light scattering during a
198   winter season in Beijing, Atmos. Environ., 110, 36–44, https://doi.org/10.1016/j.atmosenv.2015.03.037, 2015.

199   Wang, Z., Wang, R., Wang, J., Wang, Y., McPherson Donahue, N., Tang, R., Dong, Z., Li, X., Wang, L., Han, Y., and Cao,
200   J.: The seasonal variation, characteristics and secondary generation of $PM_{2.5}$ in Xi'an, China, especially during
201   pollution events, Environ. Res., 212, 113388, https://doi.org/10.1016/j.envres.2022.113388, 2022.

202   Xu, H., Cao, J., Chow, J. C., Huang, R.-J., Shen, Z., Chen, L. W. A., Ho, K. F., and Watson, J. G.: Inter-annual variability
203   of wintertime $PM_{2.5}$ chemical composition in Xi'an, China: Evidences of changing source emissions, Sci. Total
204   Environ., 545–546, 546–555, https://doi.org/10.1016/j.scitotenv.2015.12.070, 2016.

205   Xu, X., Zhang, H., Chen, J., Li, Q., Wang, X., Wang, W., Zhang, Q., Xue, L., Ding, A., and Mellouki, A.: Six sources
206   mainly contributing to the haze episodes and health risk assessment of $PM_{2.5}$ at Beijing suburb in winter 2016,
207   Ecotoxicol. Environ. Saf., 166, 146–156, https://doi.org/10.1016/j.ecoenv.2018.09.069, 2018.

208   Zhang, Q., Shen, Z., Cao, J., Zhang, R., Zhang, L., Huang, R.-J., Zheng, C., Wang, L., Liu, S., Xu, H., Zheng, C., and Liu,
209   P.: Variations in $PM_{2.5}$, TSP, BC, and trace gases (NO_2, SO_2, and O_3) between haze and non-haze episodes in winter
210   over Xi'an, China, Atmos. Environ., 112, 64–71, https://doi.org/10.1016/j.atmosenv.2015.04.033, 2015.

211 Zhang, R., Jing, J., Tao, J., Hsu, S.-C., Wang, G., Cao, J., Lee, C. S. L., Zhu, L., Chen, Z., Zhao, Y., and Shen, Z.: Chemical
212   characterization and source apportionment of $PM_{2.5}$ in Beijing: seasonal perspective, Atmos. Chem. Phys., 13, 7053–
213   7074, https://doi.org/10.5194/acp-13-7053-2013, 2013.

214 Zhang, W., Liu, B., Zhang, Y., Li, Y., Sun, X., Gu, Y., Dai, C., Li, N., Song, C., Dai, Q., Han, Y., and Feng, Y.: A refined
215   source apportionment study of atmospheric $PM_{2.5}$ during winter heating period in Shijiazhuang, China, using a
216   receptor   model   coupled   with   a   source-oriented   model,   Atmos.   Environ.,   222,   117157,
217   https://doi.org/10.1016/j.atmosenv.2019.117157, 2020.

218 Zhao, P. S., Dong, F., He, D., Zhao, X. J., Zhang, X. L., Zhang, W. Z., Yao, Q., and Liu, H. Y.: Characteristics of
219   concentrations and chemical compositions for $PM_{2.5}$ in the region of Beijing, Tianjin, and Hebei, China, Atmos. Chem.
220   Phys., 13, 4631–4644, https://doi.org/10.5194/acp-13-4631-2013, 2013.